Dyes and Pigments 92 (2012) 923–928

Contents lists available at ScienceDirect

Dyes and Pigments

journal homepage: www.elsevier.com/locate/dyepig

An efficient and energy saving approach to photocatalytic degradation of opaque high-chroma methylene blue wastewater by electrocatalytic pre-oxidation

Peiqiang Li [a], Guohua Zhao [b,*], Kunjiao Zhao [b], Junxia Gao [b], Tao Wu [b]

[a] Department of Chemistry, Shandong Agricultural University, 61 Daizong Road, 271018 Tai'an, China
[b] Department of Chemistry, Tongji University, 1239 Siping Road, 200092 Shanghai, China

ARTICLE INFO

Article history:
Received 20 December 2010
Received in revised form
6 May 2011
Accepted 2 June 2011
Available online 28 June 2011

Keywords:
Opaque dye wastewater
Photocatalytic oxidation
Electrocatalytic pre-oxidation
Decoloration
Methylene blue

ABSTRACT

The opaque methylene blue (MB) dye wastewater hard to be degraded directly by photocatalytic (PC) oxidation was successfully decomposed by a new two-step process, in which electrocatalytic (EC) pre-oxidation was followed with photoelectric synergistic catalytic (PEC) oxidation. The SnO_2/TiO_2 NTs electrode was used as the anode, which simultaneously has superior EC and PC performance. In the pre-oxidation step, the opaque dye wastewater is decolorized by EC oxidation, and the wastewater becomes a light transmission system, which provides the necessary condition for PC oxidation. However, the individual EC oxidation will be of low current efficiency and high energy consumption for the decreasing of the pollutants concentration in wastewater. Thus, in second stage, the PC process was introduced, and the synergistic catalytic oxidation leads to high PEC oxidation efficiency, so that the complete mineralization of the MB dye wastewater was realized. The whole process is highly efficient and energy-saving, which opens a new avenue to degrade the high-chroma or opaque dye wastewater.

1. Introduction

With the development of printing and dyeing industry, dyes had become one of the most serious pollutants in the water environment [1–3]. The dye wastewater is difficult to be decolorized and biodegraded for its high-chroma and strong absorption property [4–6]. Moreover, it is well known that some dye wastewater and its products such as aromatic amines are highly carcinogenic [7,8]. So dye wastewater has become a major problem in the environmental pollution control field [9–12]. The traditional treatment methods (such as adsorption, cohesion, filtration, ion exchange, etc.) have been proven to be insufficient to purify dye wastewater with complete mineralization, and it is limited by its complicated post-treatment procedures. Among the new oxidation methods, photocatalysis and electrocatalysis have appeared as emerging destructive technologies owning to their total mineralization of many organic pollutants [13–15]. So the photocatalytic (PC) and electrocatalytic (EC) oxidation has been attracted more concern in the dye wastewater treatment [16–18].

Previous studies showed that electron transfer between dyes and nanosized semiconductor particles occurs under visible and UV irradiation, and the dyes can be degraded to smaller molecules and ultimately mineralized completely to water, carbon dioxide and other inorganic ions. Among heterogeneous photocatalyst TiO_2 is widely applied to purify the dye wastewater [19–22]. PC degradation of dyes has been realized by TiO_2 thin films or suspensions. Among all forms of TiO_2 the TiO_2 NTs array with a highly ordered arrangement is effective on dye wastewater owning to its high specific surface area, adsorption capacity and more active sites [23–26]. However, all the PC oxidation works on the premise that the aqueous solution should be transparent or have certain light transmittance, so the PC degradation is only suitable for the dye wastewater with low concentration and certain light transmission. And individual PC oxidation often fails to treat the dye wastewater with high concentration and deep color.

EC oxidation is also an efficient pollution control technology [27–31]. At a certain potential, the pollutant on the electrode surface can be oxidized. However, the reaction probability will decrease with the descent of the initial pollutant concentration due to the evolution of oxygen and hydrogen as side reaction. So the current efficiency decreases rapidly and the energy consumption increases. Therefore, EC oxidation is very suitable for the pretreatment of the high chroma wastewater, which will supply necessary condition for the PC oxidation.

According to the above analysis, we propose a sectional degradation of high-chroma dye wastewater. Individual EC

* Corresponding author. Fax: +86 (0)538 8242251.
E-mail addresses: pqli@sdau.edu.cn (P. Li), g.zhao@tongji.edu.cn (G. Zhao).

0143-7208/$ – see front matter © 2011 Elsevier Ltd. All rights reserved.
doi:10.1016/j.dyepig.2011.06.009

oxidation can be firstly applied to destruct the chromophore of the pollutant and decrease the colority, and the transmittance of the dye wastewater will be increased by the EC pre-oxidation. However, EC oxidation will be at low current efficiency and need high electrochemical energy consumption with the decrease of pollutants concentration. Then, the role of the photocatalyst will bring into play. Nevertheless, the individual PC or EC is not efficient enough. So the photoelectric synergistic catalytic oxidation can be adopted to achieve high efficient catalytic oxidation at the second stage. It is expected that this two-section treatment might be efficient and energy-saving. An intensive research on the feasibility, efficiency, energy consumption of this process is carried out. As we known, the material and the properties of the anode are crucial to the efficient degradation of the high-chroma dye wastewater. And the anode must own both high EC and PC oxidation ability. In fact, the Sb-doped SnO_2/TiO_2 NT anode prepared in our previous research happens to meet this requirement and might act as a qualified material [32]. It inherits good PC oxidation properties of TiO_2 NTs, and the photoconversion efficiency is 26.1%, which is much higher than 8.2% of the TiO_2 NTs. It also owns excellent EC oxidation property of the Sb-doped SnO_2/Ti. Moreover, it presents high efficiency on the degradation of refractory aromatic acid [32].

The novelty of this research is the sectional degradation of opaque methylene blue (MB) dye wastewater. Such a sectional treatment commendably realizes the efficient degradation of opaque dye wastewater. The reason of the efficiency and energy-saving is discussed from the reaction kinetics and the energy consumption.

In this study, high chroma MB solution (100 mg L^{-1}) is selected as the target pollutant. The molecular structure of MB contains a benzene ring, accompanied with N and S hetero-atom. It also is a refractory organic matter and can cause serious harm to the environment [33–35]. The application of the new two-step process to degrade MB dye wastewater will provide a new method for the degradation of deep colored or opaque dyes wastewater.

2. Experimental section

2.1. Materials

Titanium sheets (thickness 1 mm, purity 99.8%) was purchased from Jucheng Titanium Sheets Corporation in Baoji, China. MB, anhydrous sodium sulfate, stannous chloride, antimony trichloride and polyethylene glycol 400 were of analytical grade (Sinopharm Chemical Reagent Co. Ltd). All the solutions were prepared using deionized water.

The TiO_2 NTs were first prepared by the electrochemical anodic oxidation with the pretreated titanium sheets as anode. Then, the vacuum treated TiO_2 NTs were immersed into tin-antimony sol-gel and annealed to obtain the Sb-doped SnO_2/TiO_2 NTs (SnO_2/TiO_2 NTs) anode [32].

2.2. Photoelectric degradation experiment and analysis

Photoelectric degradation experiment was carried out in a single circular electrochemical reaction cell, externally connected to circulating water to keep the reaction at a constant temperature of 25 °C. SnO_2/TiO_2 NTs works as the anode, and titanium as cathode (Schematic diag. 1). The electrode area is 4.5 cm^2 with the gap of 1.0 cm, and the current density is 30 mA cm^{-2}. 100 mg L^{-1} MB solution containing 0.1 M Na_2SO_4 is used as the simulated wastewater, and the solution volume is 100 mL. 300 W UV lamp (center wavelength 365 nm, light intensity 3 mW cm^{-2}) is the light source.

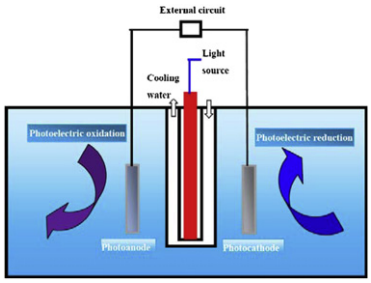

Schematic diag. 1. Schematic diagram of EC, PC and PEC experimental setup.

UV–vis spectrophotometer (Agilent 8453, Agilent Corporation, USA) was used to determine the absorbance (A) and transmittance (T) of the solution before and after reaction, measuring the absorbance of the MB solution at the maximum absorption wavelength ($\lambda = 664$ nm). The decoloration ratio is calculated as follows [36]:

$$\text{Decoloration ratio} = \left(A_{\text{before}} - A_{\text{after}}\right) \Big/ A_{\text{before}} \times 100\% \quad (1)$$

where A_{before} and A_{after} is the absorbance of the solution before and after reaction.

The concentration of MB were measured by HPLC (Agilent HP 1100, Agilent Corporation, USA) with Ultimat TMAQ-C18 (4.6 × 100 mm, 5 μm) at 25 °C and selected UV detector at $\lambda = 292$ nm. 60:40 (v/v) methanol/phosphate buffer (pH = 2.3) was employed as the mobile phase at the flow rate of 1.0 mL min^{-1}. 20 μL aliquots were injected into the HPLC sampler. The sample was filtered through a microporous filter (13 mm × 0.20 mm) before each analysis.

Total organic carbon (TOC) was measured on a Shimadzu TOC-Vcpn analyzer. The mineralization reaction of MB is as follows:

$$2C_{16}H_{18}ClN_3S_2 + 80H_2O \rightarrow 32CO_2 + Cl_2 + 4SO_4^{2-} + 3N_2 + 196H^+ + 188e^- \quad (2)$$

Mineralization current efficiency (MCE) at a given time t for the treated MB solution is estimated as follows [37]:

$$\text{MCE} = \frac{\Delta(\text{TOC})_{\text{exp}}}{\Delta(\text{TOC})_{\text{theor}}} \times 100\% \quad (3)$$

where $\Delta(\text{TOC})_{\text{exp}}$ is the experimental value for TOC removal at time t, and $\Delta(\text{TOC})_{\text{theor}}$ is the theoretically value of TOC removal, calculated by

$$\Delta(\text{TOC})_{\text{theor}} = \frac{\dfrac{I \times t}{n_e \times F} \times n_c \times M \times 10^3}{V} \text{mg L}^{-1} \quad (4)$$

where I is the current intensity (A), t is electrolysis time (s), F is Faraday constant, $F = 96{,}485$ C mol^{-1}, n_e is the electron transfer number in equation (1), n_c is the carbon number of the organic compound, M is carbon atomic weight, 12 g mol^{-1}, and V is the volume of the sample solution (L). For MB, n_e and n_c are 188 and 16, respectively.

The energy consumption in the single EC and PEC processes is calculated as follows [38]:

$$E = \frac{UIt}{V\log(C_0/C_t)} \quad (5)$$

where U is the voltage (V), I is the current intensity (A), t is the degradation time (s), V is the volume of the sample solution (L), C_0 and C_t are the concentrations of MB at time 0 and t (mg L^{-1}).

The energy consumption in the single PC process is calculated as follows:

$$E = Pt \quad (6)$$

where P is the power of the UV light source, and t is the degradation time (s).

For the two-step process, the energy consumption equals to the sum of the energy in each step.

3. Results and discussion

3.1. The suitable reaction condition for the PEC oxidation: EC pre-oxidation

The SnO_2/TiO_2 NTs anode used in the experiment is an electrode owns both high EC and PC oxidation efficiency. It inherits the good PC oxidation properties of TiO_2 NTs, the photoconversion efficiency is 26.1%, much higher than 8.2% of the TiO_2 NTs [32]. It also inherits the excellent EC oxidation properties of the Sb-doped SnO_2/Ti, and the oxygen evolution potential is as high as 1.8 V versus saturated calomel electrode (SCE). Therefore, it is suitable for the photo-electrocatalytic (PEC) degradation of organic contaminants.

The light transmittance rate of the initial 100 mg L^{-1} MB was almost zero. Fig. 1A shows the light transmittance ratio of the MB solution changing with time. It can be seen that the light transmittance rate of the solution increased from zero to 2.8% after 9 h with the single PC oxidation treatment. The decoloration rate of the solution is determined by the absorbance at characteristic absorption band of MB ($\lambda = 664$ nm). The decoloration ratio is only 13% after 9 h PC oxidation (Fig. 1B), so the individual PC oxidation exhibited poor decoloration effect. Fig. 2a depicts the UV–visible absorption spectra during the degradation of MB in the PC process. It also shows that MB is hard to be degraded by individual PC oxidation. And TOC decreases slowly in the whole PC oxidation process, which is still at a high value of 47.1 mg L^{-1} with TOC removal of 12.0% after 6 h (Fig. 3a). Many studies of the MB PC degradation is based on the MB concentration is very low. In Ammar Houas and Tai Cheng An's study, the research concentration is 0.072 and 1 mmol L^{-1} [34,39]. In this study, 100 mg L^{-1} converted

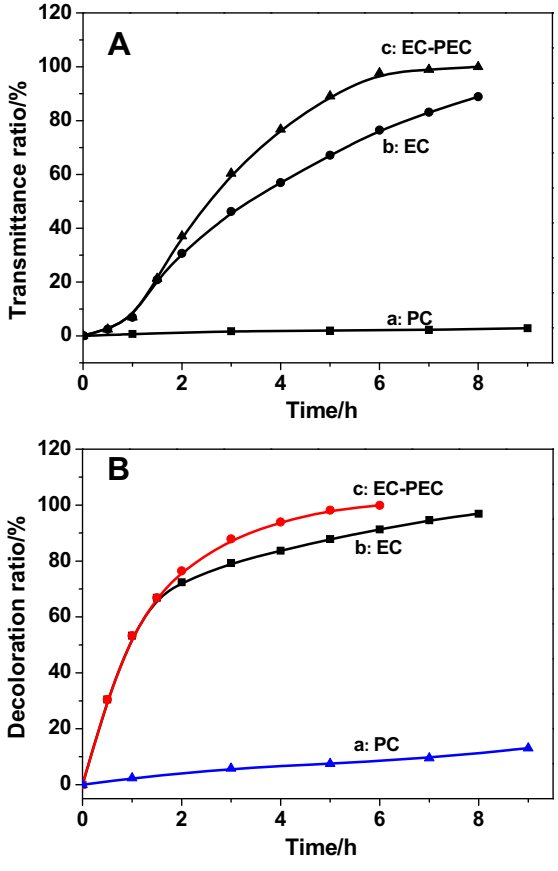

Fig. 1. A: The transmittance ratio of the MB solution changes with time in PC (a), EC (b) and PC-PEC (c) processes. B: Decoloration rate of the MB solution vs. time in PC (a), EC (b) and PC-PEC (c) processes.

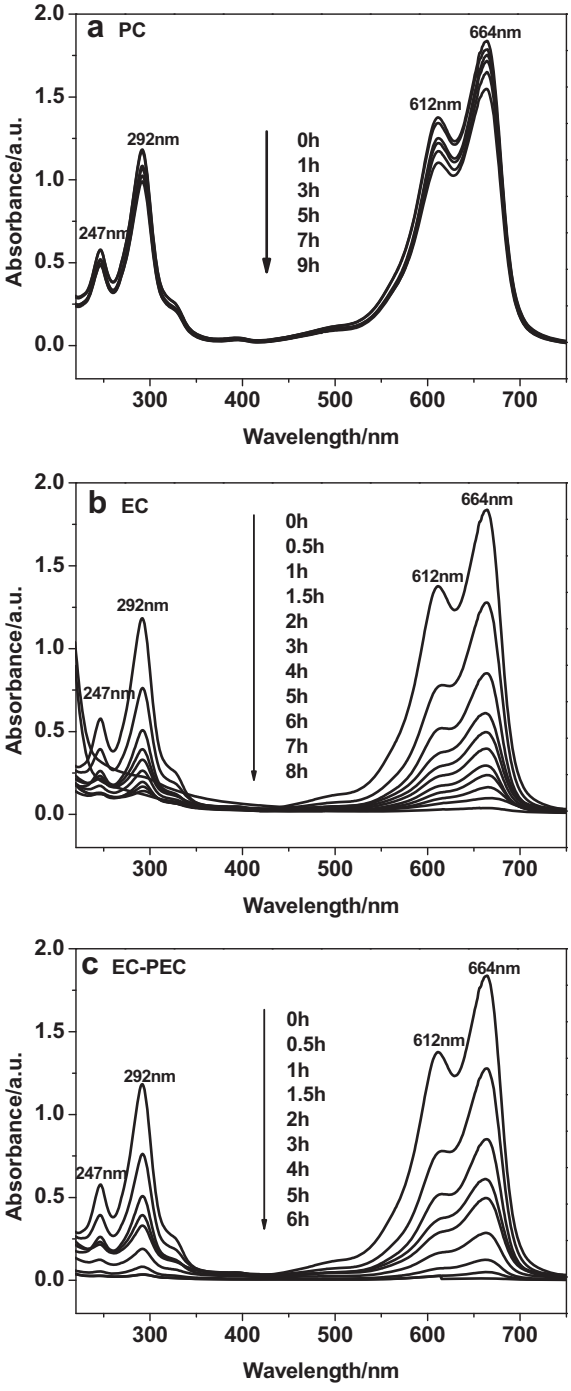

Fig. 2. The UV–visible absorption spectra of MB solution in PC (a), EC (b) and PC-PEC (c) processes.

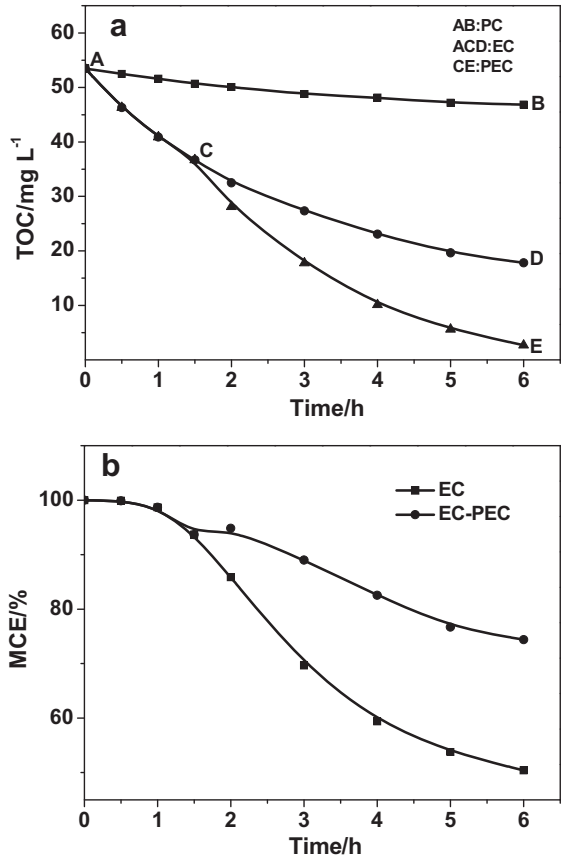

Fig. 3. a): The TOC variation of MB with time in PC, EC and PC-PEC processes. b): The MCE variation with time in EC and PC-PEC processes.

to molar concentration is 28 mmol L^{-1}. So high-chroma MB could not be degraded effectively by individual PC oxidation, because light could not penetrate the dye solution for the deep color, and the PC reaction probability is further decreased for the strong adsorption of MB on the electrode surface, this leads to that the PC oxidation does not have function on the opaque MB solution.

As respect to EC oxidation, no special requirements for the light transmittance of the solution, and good results can be obtained for the degradation of the dye wastewater. Thus, EC oxidation is suitable for the pretreatment of the opaque MB solution to improve its light transmittance. It shows that the light transmittance ratio increases rapidly to 20.9% at 1.5 h (Fig. 1A, curve b) and the decoloration ratio is up to 67.1% at 1.5 h (Fig. 1B, curve b), indicating that EC oxidation can efficiently decrease the colority and increase the transmittance ratio of the MB solution.

Fig. 2b presents the UV–visible spectra of MB solution change with the time in the EC process. The maximal absorption band occurred at 247, 292, 612 and 664 nm (Fig. 2). The bands at 247 and 292 nm are from the benzene ring conjugated system, and the bands at 612 and 664 nm are from the MB chromophore ring structure (phenothiazine or thionine). The latter bands gradually decrease with time, indicating that the MB solution is decolorized. It can be explained from two aspects: One is that demethylation and deamination oxidative degradation take place during the EC oxidation of MB, it is consistent with the wide bands between 612 and 664 nm (Fig. 2). As weak electron-donor substituent, methyl groups can be easily attacked by electrophilic species in the demethylation process [35]. The color of MB solution will become less intense (hypsochromic effect) when all or part of the auxochromic groups (methyl or methylamine) are degraded. The other reason is the cleavage of bonds between the C–S^+=C functional chromophore group in MB which causes the definitive dissociation of the two benzene rings, and further leads to the hypsochromic effect [34]. It indicates that EC oxidation provides appropriate condition for the subsequent PC oxidation because the colority of MB solution is decreased.

Moreover, the organic carbon in the solution is degraded in the EC process. At 1.5 h, the TOC reduced 31.8% (Fig. 3a). It could be correspond to the aromatic ring opening with the transient formation of carboxylic acids followed by the evolution of CO_2. It can be seen that the TOC in the solution first decreases obviously (Fig. 3a, part AC) and then decreases slowly (Fig. 3a, part CD). This can be well explained by the MCE, the MCE is high at the beginning of the reaction (in the first 1.5 h), which are more than 90%. But the MCE rapidly decreases later (Fig. 3b), which is only 50% at 6 h leading to the poor treatment effect, and the energy consumption correspondingly increases with TOC removal (Fig. 4). The colority of MB solution is reduced in a short time and the light transmittance of solution is increased with EC oxidation, which indicated that EC is more suitable for the pretreatment and provide appropriate conditions for subsequent PC process. However, the current efficiency is low and energy consumption is high in the latter stage, so the EC oxidation is not suitable for the pollutant with low concentration.

3.2. High efficient and energy saving of the two-step process

Since the current efficiency in the EC process decreases rapidly and its energy consumption increases with the decreasing of MB concentration, PC is introduced at 1.5 h to form a photoelectrocatalytic (PEC) oxidation for the system in order to maintain high degradation efficiency.

Firstly, the degradation kinetics of MB in the two-step process was studied. It found that the logarithm of MB concentration (ln*C*) has a good linear relationship with the reaction time (*t*). It indicates that the MB decay fits to a pseudo first-order reaction in EC, PC and PEC processes, and the apparent rate constant k_s is 0.56, 0.04 and 1.86 h^{-1} (Fig. 5b), respectively. In the two-step process, MB is completely degraded at 4 h, which is divided into two stages. The first 1.5 h is the EC process with k_s of 0.56 h^{-1}. When UV light is introduced at 1.5 h to initiate PC oxidation reaction, due to the excellent PC and EC performance of the electrode, MB is rapidly degraded in the PEC process, so that the rate constant increases to 1.56 h^{-1} (Fig. 5b), which is 2.8 times higher than that in the single EC process. This proves that the degradation of MB is faster and more efficient in the two-step process.

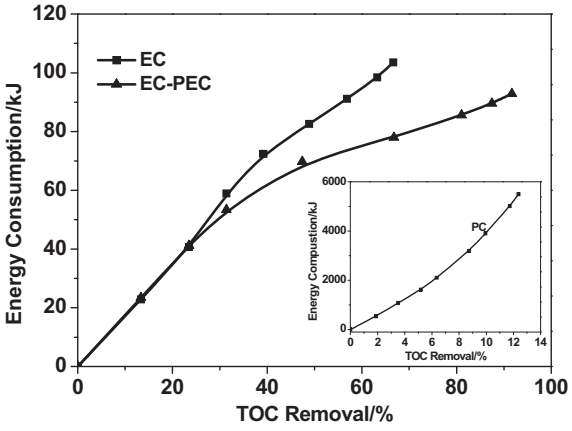

Fig. 4. The energy consumption variation with TOC removal in PC, EC and PC-PEC processes.

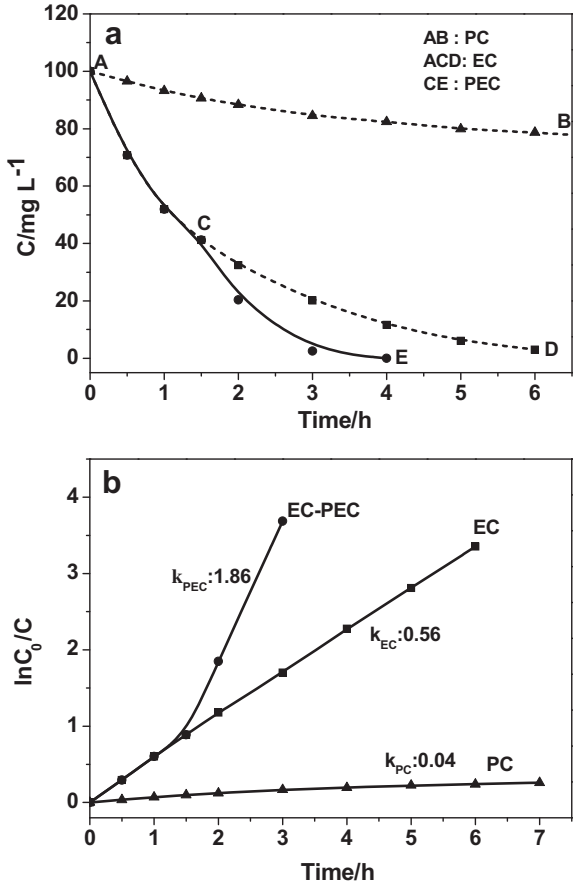

Fig. 5. a): The concentration variation of MB with time in PC, EC and PC-PEC processes. b): The apparent rate constant variation with time in PC, EC and PC-PEC processes.

The peaks of MB at 612 and 664 nm decreased greatly from 1.5 to 6 h (Fig. 2c). This indicates that the bonds of the C–S^+=C functional chromophore group is destructed to a further extent than the EC process (Fig. 2b), and the peaks at 247 and 292 nm decreased greatly, indicating that the benzene ring is also further destructed (Fig. 2c), which can be markedly reflected by the TOC removal and the calculated MCE. It can be seen that MCE is less than 85.9% after 1.5 h (Fig. 3b) in the EC process, and it decreases to 50.4% at 6 h (Fig. 3b), this is ascribed to the decreasing of pollutants concentration and the increasing of the side reactions on the electrode. So the MCE decreases greatly in this process. In order to maintain higher efficiency, the PC oxidation is introduced at 1.5 h (Fig. 3a, point C) and the PEC oxidation continues (Fig. 3a, CE section). It can be seen that MCE changes from 94.0% at 1.5 h to 74.4% at 6.0 h in the PEC process, while it changed from 94.0% to 50.4% in the EC process, respectively. So the oxidation efficiency is improved greatly in the PEC process than that in the single EC process. It can be further proved by the TOC removal. Fig. 3a shows that TOC of the MB solution decreases greatly from 1.5 to 6 h in CE section (PEC process), and it is 2.7 mg L^{-1} at 6 h, which is much lower than the EC process (17.8 mg L^{-1}) (Fig. 3a). Thus the PEC oxidation can keep good degradation results for low pollutant concentrations in the second stage.

The treatment results of PEC process are much better than the EC process. On the one hand, MB and its intermediates are adsorbed on the anode which leads to the decrease of the UV absorption. On the other hand, the adsorption of them on the electrode can result in the fouling of the EC sites. The two aspects result in the drop of oxidation efficiency. Oppositely, the intermediates on this anode are removed by EC process, which can enhance the absorption of UV and accelerate the PC process. Similarly, the photo-generated holes and the radicals such as ·OH produced in the PC process are helpful to remove the intermediates, thus alleviates the fouling of the electrode. The enhancement of the EC process is also realized. So the synergistic interaction of PC and EC in the PEC process achieved good treatment efficiency for MB than the individual EC process. The results are in accordance with the earlier study [32].

At the same time, energy consumption was compared among the PC, EC and EC-PEC processes (Fig. 4). It can be seen that the individual PC process costs more energy with very low TOC removal (Fig. 4, inset map). In the EC process, it costs 103.7 kJ at the TOC removal of 66.8%, and in the EC-PEC process it costs 93.1 kJ at the TOC removal of 92.2%. Therefore, the two-step process proposed is a highly efficient and energy-saving degradation technology for high-chroma and opaque MB solution.

4. Conclusion

A two-step process for the degradation of the high-chroma and opaque MB dye wastewater was proposed in this paper, and complete mineralization of MB was successfully achieved on the SnO_2/TiO_2 NTs anode, which possessed superior EC and PC performance. In the pre-oxidation process, the opaque dye wastewater was decolorized with EC oxidation, and became a light transmission system, which provided the necessary condition for PC oxidation. To solve the problem of the EC oxidation with low current efficiency and high energy consumption for the decreasing of the concentration in wastewater, the PC oxidation was introduced. The synergistic catalytic oxidation leaded to high PEC oxidation efficiency, so that it achieved the complete mineralization of dye wastewater. In the two-step process it costs 93.1 kJ at the TOC removal of 92.2%, it costs less energy, but it achieves better treatment effect, so the whole process was proved to be efficient and energy-saving, which opens a new avenue to degrade the high-chroma and opaque dye wastewater.

Acknowledgments

This work was supported jointly by the National Natural Science Foundation of China (Project NO.20877058), 863 Program (Project NO.2008AA06Z329) from the Ministry of Science, and Nanometer Science Foundation of Shanghai (Project NO. 0852nm01200).

References

[1] Konstantinou IK, Albanis TA. TiO2-assisted photocatalytic degradation of azo dyes in aqueous solution: Kinetic and mechanistic investigations – a review. Appl Catal B-Environ 2004;49:1–14.
[2] Wu TX, Liu GM, Zhao JC, Hidaka H, Serpone N. Photoassisted degradation of dye pollutants. V. Self-photosensitized oxidative transformation of Rhodamine B under visible light irradiation in aqueous TiO_2 dispersions. J Phys Chem B 1998;102:5845–51.
[3] Mrowetz M, Selli E. Effects of iron species in the photocatalytic degradation of an azo dye in TiO_2 aqueous suspensions. J Photochem Photobiol A 2004;162:89–95.
[4] Yi FY, Chen SX, Yuan C. Effect of activated carbon fiber anode structure and electrolysis conditions on electrochemical degradation of dye wastewater. J Hazard Mater 2008;157:79–87.
[5] Fan J, Guo YH, Wang JJ, Fan MH. Rapid decolorization of azo dye methyl orange in aqueous solution by nanoscale zerovalent iron particles. J Hazard Mater 2009;166:904–10.
[6] Zhuang X, Wan Y, Feng CM, Shen Y, Zhao DY. Highly efficient adsorption of bulky dye molecules in wastewater on ordered mesoporous carbons. Chem Mater 2009;21:706–16.
[7] Khalid A, Arshad M, Crowley DE. Biodegradation potential of pure and mixed bacterial cultures for removal of 4-nitroaniline from textile dye wastewater. Water Res 2009;43:1110–6.
[8] Chou PH, Matsui S, Misaki K, Matsuda T. Isolation and identification of xenobiotic aryl hydrocarbon receptor ligands in dyeing wastewater. Environ Sci Technol 2007;41:652–7.

[9] Akhtar S, Khan AA, Husain Q. Potential of immobilized bitter gourd (Momordica charantia) peroxidases in the decolorization and removal of textile dyes from polluted wastewater and dyeing effluent. Chemosphere 2005;60:291–301.
[10] Chen ZX, Li DZ, Zhang WJ, Shao Y, Chen TW, Sun M, et al. Photocatalytic degradation of dyes by $ZnIn_2S_4$ microspheres under visible light irradiation. J Phys Chem C 2009;113:4433–40.
[11] Chen WX, Lu WY, Yao YY, Xu MH. Highly efficient decomposition of organic dyes by aqueous-fiber phase transfer and in situ catalytic oxidation, using fiber-supported cobalt phthalocyanine. Environ Sci Technol 2007;41:6240–5.
[12] Lin J, Gao HW. SDBS@$BaSO_4$: an efficient wastewater-sorbing material. J Mater Chem 2009;19:3598–601.
[13] Bavykin DV, Friedrich JM, Walsh FC. Protonated titanates and TiO_2 nanostructured materials: synthesis, properties, and applications. Adv Mater 2006;18:2807–24.
[14] An HQ, Zhu BL, Li JX, Zhou J, Wang SR, Zhang SM, et al. Synthesis and characterization of thermally stable nanotubular TiO_2 and its photocatalytic activity. J Phys Chem C 2008;112:18772–5.
[15] Sohn YS, Smith YR, Misra M, Subramanian V. Electrochemically assisted photocatalytic degradation of methyl orange using anodized titanium dioxide nanotubes. Appl Catal B-Environ 2008;84:372–8.
[16] Li GT, Qu JH, Zhang XW, Ge JT. Electrochemically assisted photocatalytic degradation of Acid Orange 7 with beta-PbO_2 electrodes modified by TiO_2. Water Res 2006;40:213–20.
[17] Hachem C, Bocquillon F, Zahraa O, Bouchy M. Decolourization of textile industry wastewater by the photocatalytic degradation process. Dyes Pigments 2001;49:117–25.
[18] Muruganandham M, Swaminathan M. Photocatalytic decolourisation and degradation of Reactive Orange 4 by TiO_2-UV process. Dyes Pigments 2006;68:133–42.
[19] Liu CC, Hsieh YH, Lai PF, Li CH, Kao CL. Photodegradation treatment of azo dye wastewater by UV/TiO_2 process. Dyes Pigments 2006;68:191–5.
[20] Kuo WS, Ho PH. Solar photocatalytic decolorization of dyesin solution with TiO_2 film. Dyes Pigments 2006;71:212–7.
[21] Sahoo C, Gupta AK. Anjali Pal Photocatalytic degradation of Crystal Violet (C.I. Basic Violet 3) on silver ion doped TiO_2. Dyes Pigments 2005;66:189–96.
[22] Jin YN, Wu MF, Zhao GH, Li MF. Photocatalysis-enhanced electrosorption process for degradation of high-concentration dye wastewater on TiO_2/carbon aerogel. Chem Eng J 2011;168:1248–55.
[23] Prado AGS, Costa LL. Photocatalytic decouloration of malachite green dye by application of TiO_2 nanotubes. J Hazard Mater 2009;169:297–301.
[24] Zhang ZH, Yuan Y, Shi GY, Fang YJ, Liang LH, Ding HC, et al. Photoelectrocatalytic activity of highly ordered TiO_2 nanotube arrays electrode for azo dye degradation. Environ Sci Technol 2007;41:6259–63.
[25] Zhang JL, Zhou BX, Zheng Q, Li JH, Bai J, Liu YB, et al. Photoelectrocatalytic COD determination method using highly ordered TiO_2 nanotube array. Water Res 2009;43:1986–92.
[26] Zlamal M, Macak JM, Schimuki P, Krysa J. Electrochemically assisted photocatalysis on self-organized TiO_2 nanotubes. Electrochem Commun 2007;9:2822–6.
[27] Zhao GH, Gao JX, Shi W, Liu MC, Li DM. Electrochemical incineration of high concentration azo dye wastewater on the in situ activated platinum electrode with sustained microwave radiation. Chemosphere 2009;77:188–93.
[28] Shen ZM, Wu D, Yang J, Yuan T, Wang WH, Jia JP. Methods to improve electrochemical treatment effect of dye wastewater. J Hazard Mater 2006;131:90–7.
[29] Mohan N, Balasubramanian N. In situ electrocatalytic oxidation of acid violet 12 dye effluent. J Hazard Mater 2006;136:239–43.
[30] Mohan N, Balasubramanian N, Basha CA. Electrochemical oxidation of textile wastewater and its reuse. J Hazard Mater 2007;147:644–51.
[31] Lv GF, Wu DC, Fu RW. Performance of carbon aerogels particle electrodes for the aqueous phase electro-catalytic oxidation of simulated phenol wastewaters. J Hazard Mater 2009;165:961–6.
[32] Li PQ, Zhao GH, Cui X, Zhang YG, Tang YT. Constructing stake structured TiO_2-NTs/Sb-Doped SnO_2 electrode simultaneously with high electrocatalytic and photocatalytic performance for complete mineralization of refractory aromatic acid. J Phys Chem C 2009;113:2375–83.
[33] Almeida CAP, Debacher NA, Downs AJ, Cottet L, Mello CAD. Removal of methylene blue from colored effluents by adsorption on montmorillonite clay. J Colloid Interf Sci 2009;332:46–53.
[34] Houas A, Lachheb H, Ksibi M, Elaloui E, Guillard C, Herrmann JM. Photocatalytic degradation pathway of methylene blue in water. Appl Catal B-Environ 2001;31:145–57.
[35] Zhang TY, Oyama T, Aoshima A, Hidaka H, Zhao JC, Serpone N. Photooxidative N-demethylation of methylene blue in aqueous TiO_2 dispersions under UV irradiation. J Photochem Photobiol A 2001;140:163–72.
[36] Korbahti BK, Rauf MA. Determination of optimum operating conditions of carmine decoloration by UV/H_2O_2 using response surface methodology. J Hazard Mater 2009;161:281–6.
[37] Brillas E, Boye B, Sires I, Garrido JA, Rodriguez RM, Arias C, et al. Electrochemical destruction of chlorophenoxy herbicides by anodic oxidation and electro-Fenton using a boron-doped diamond electrode. Electrochim Acta 2004;49:4487–96.
[38] Bolton JR, Bircher KG, Tumas W, Tolman CA. Figures-of-merit for the technical development and application of advanced oxidation technologies for both electric- and solar-driven systems – (IUPAC Technical Report). Pure Appl Chem 2001;73:627–37.
[39] An TC, Zhu XH, Xiong Y. Feasibility study of photoelectrochemical degradation of methylene blue with three-dimensional electrode-photocatalytic reactor. Chemosphere 2002;46:897–903.